Electronic Supplementary Information to

Oximate metal complexes breaking the limiting esterolytic reactivity of oximate anions

Paola Gómez-Tagle, José Carlos Lugo-González and Anatoly K. Yatsimirsky*
Universidad Nacional Autónoma de México, Facultad de Química, 04510, Mexico City, Mexico.
E-mail: anatoli@unam.mx; Fax: +52 55 56162010; Tel: +52 55 56223813

Synthesis and characterization of the ligand 1.

Ligand 1 was obtained by a condensation in diisopropyl ether followed by a reduction in methanol. A solution of 20 mmol (2.02 g) of recrystallized 2,3-butanedione monoxime and 20 mmol (2.25 mL) of 2-aminomethyl pyridine was stirred and heated at 60°C during 2 h. The solid product was filtered off, washed with isopropyl ether and air-dried. Yield 3.37 g, 88%. For the imine reduction, 80 mmol of sodium tetrahydroborate (3.03 g), dissolved in the minimum volume of methanol, was added dropwise to a solution of 17.5 mmol of the imine (3.3 g) in 50 mL of methanol cooled and stirred on an ice bath. The mixture was stirred 1 h at room temperature and the product is obtained as a pale yellow oil after the methanol was removed under vacuum. This oil was dissolved in 20 mL of CH_2Cl_2, and precipitated usually as **1**·2HCl salt by bubbling HCl (g) thorough the solution. The final product was filtered off, washed with cold CH_2Cl_2 and stored in a dessicator. Yield 2.94 g, 63%.
IR (DRIFT, ν_{max} in cm^{-1}): 3302 (m), 3051 (w), 3009 (w), 2793 (w), 2875 (w), 2605 (s), 2368 (w), 2245 (w), 2178 (w), 2134 (w), 2053 (m), 1989 (m), 1940 (m), 1870 (m), 1663 (s), 1636 (s), 1617 (s), 1582 (s), 1547 (s), 1474 (m), 1440 (m), 1420 (m), 1392 (m), 1332 (m), 1314 (m), 1287 (s), 1224 (s), 1160 (s), 1125 (s), 1100 (m), 1062 (s), 1047 (m), 1026 (m), 993 (m), 946 (s), 800 (m), 781 (s), 660 (m), 628 (s), 596 (s), 505 (s), 483 (s).
^{1}H NMR (300 MHz, DMSO-d6) δ 11.32 (s, 1H), 8.74 (dd, J= 5.2, 0.9Hz, 1H), 8.15 (td, J=7.8, 1.7Hz 1H), 7.95 (d, J= 7.9Hz, 1H), 7.65 (m, 1H), 4.33 (m, 2H), 3.96 (q, J=6.5Hz, 1H); 1.89 (s, 3H), 1.49 (d, J=6.9Hz, 3H);
^{13}C NMR (75 MHz, DMSO-d6) δ 157.82, 156.39, 147.97, 139.02, 122.79, 120.57, 55.79, 51.28, 18.03, 14.59.
MS (EI, *m/z*) 193 [M^+; calcd for $C_{10}H_{15}N_3O$: 193.12].

Anal. Cal. for **1**·2HCl: C, 45.12; H, 6.44; N, 15.79. Found: C, 45.21; H, 5.7; N, 15.87.

Potentiometric and spectrophotometric titrations.

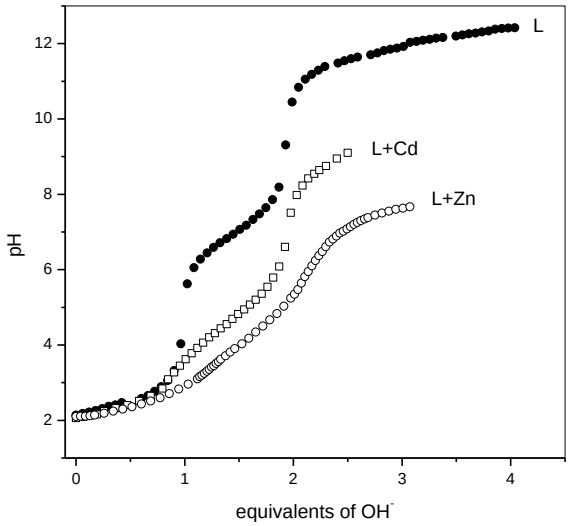

Figure S1. Potentiometric titration of 8.8 mM **1**·2HCl alone (solid circles) and in the presence of 10 mM Cd(II) (open squares) or Zn(II) (open cirles). Titrations with metal ions were terminated at the moment of beginning of precipitation. Four additional titrations with different metal and ligand concentrations in the range from 5 to 10 mM were performed.

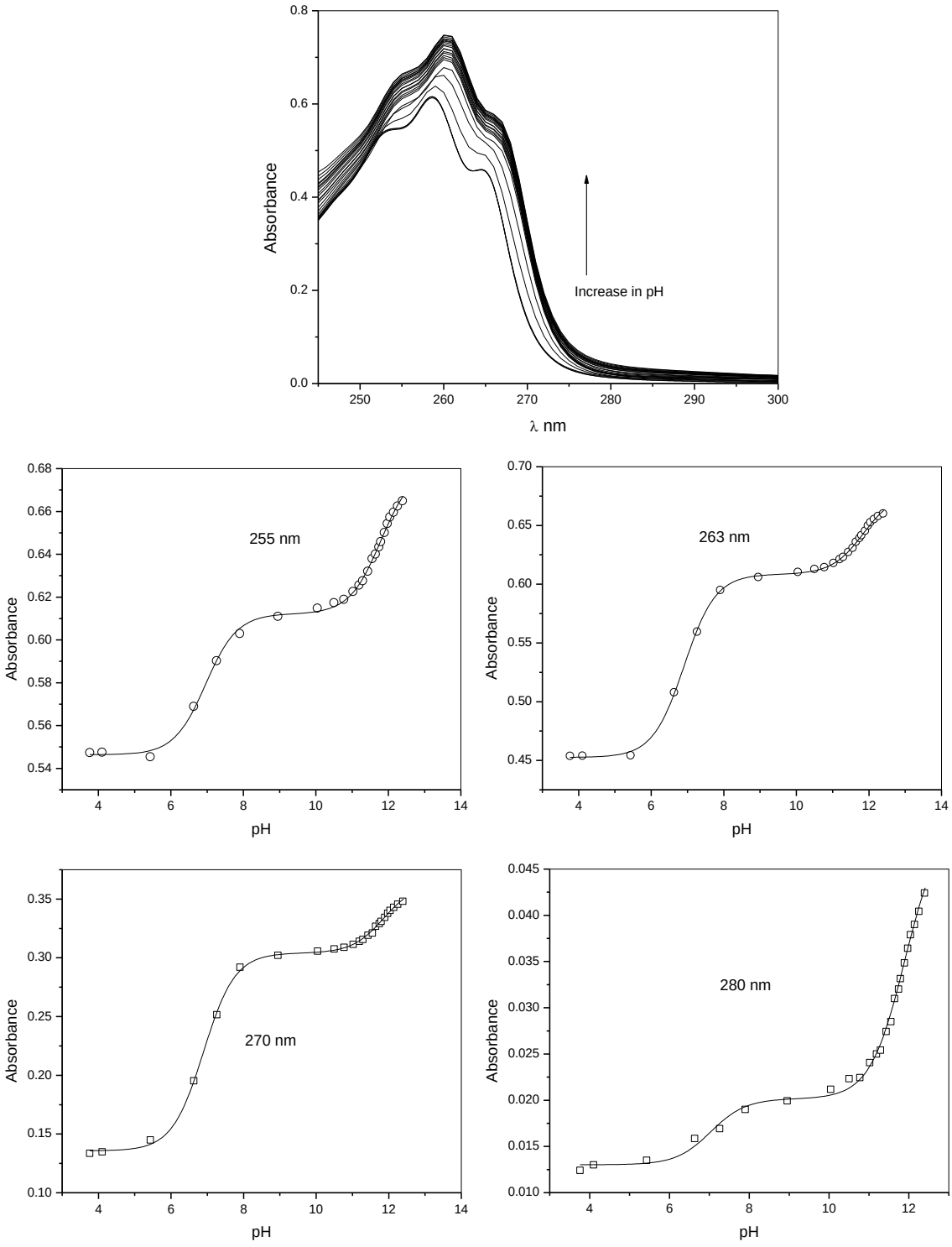

Figure S2. Absorption spectra of 0.2 mM **1** in the range of pH 3.7-12.4 and plots of absorbance vs. pH at selected fixed wavelengths. Data at wavelengths below 245 nm were not analyzed because of interference from pH-variable absorption of the buffer (mixture of 0.01 M MES, MOPS and CAPS) and are not shown in the figure.

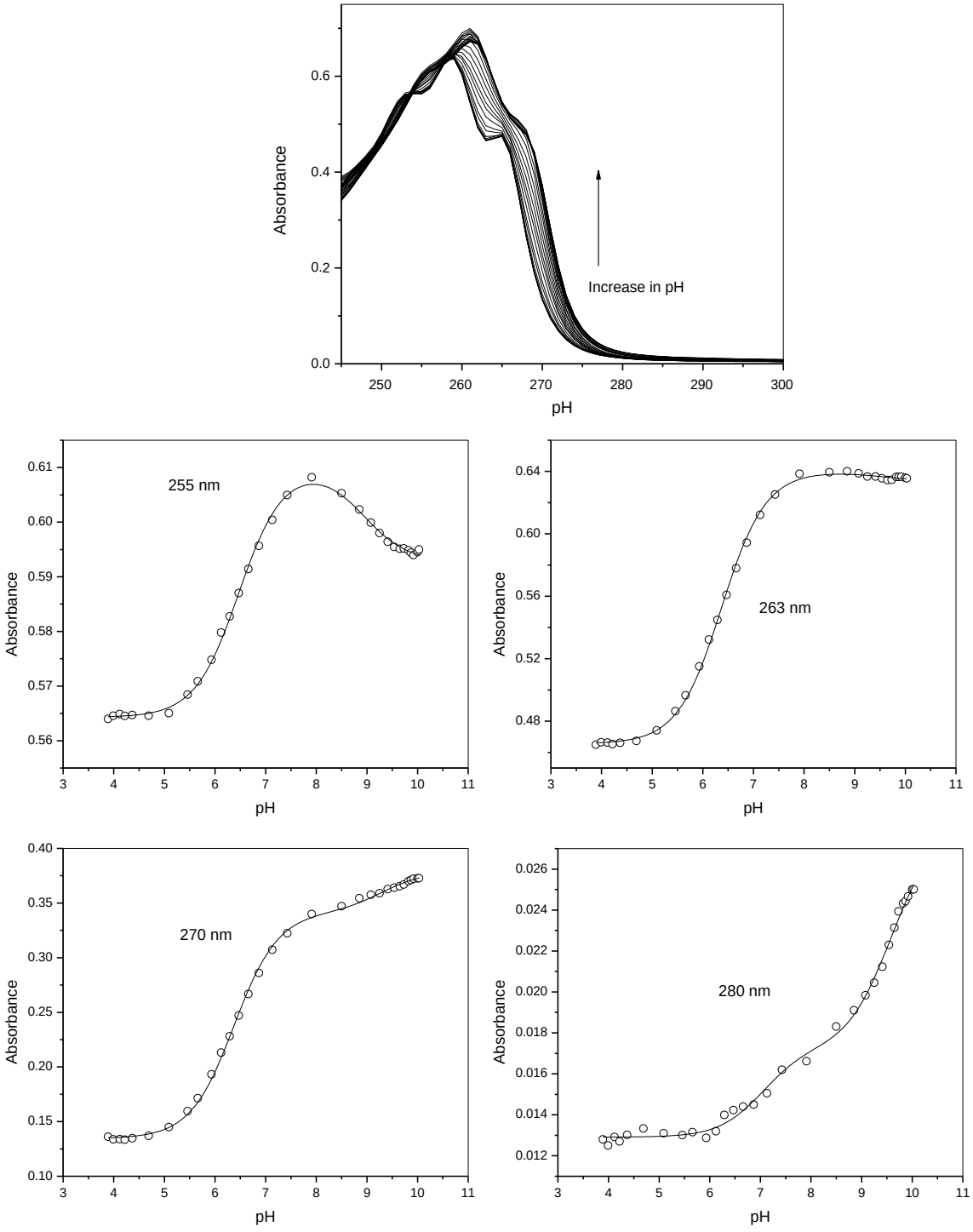

Figure S3. Absorption spectra of the mixture of 0.2 mM **1** and 0.2 mM Cd(II) in the range of pH 3.9-10.0 and plots of absorbance vs. pH at selected fixed wavelengths.

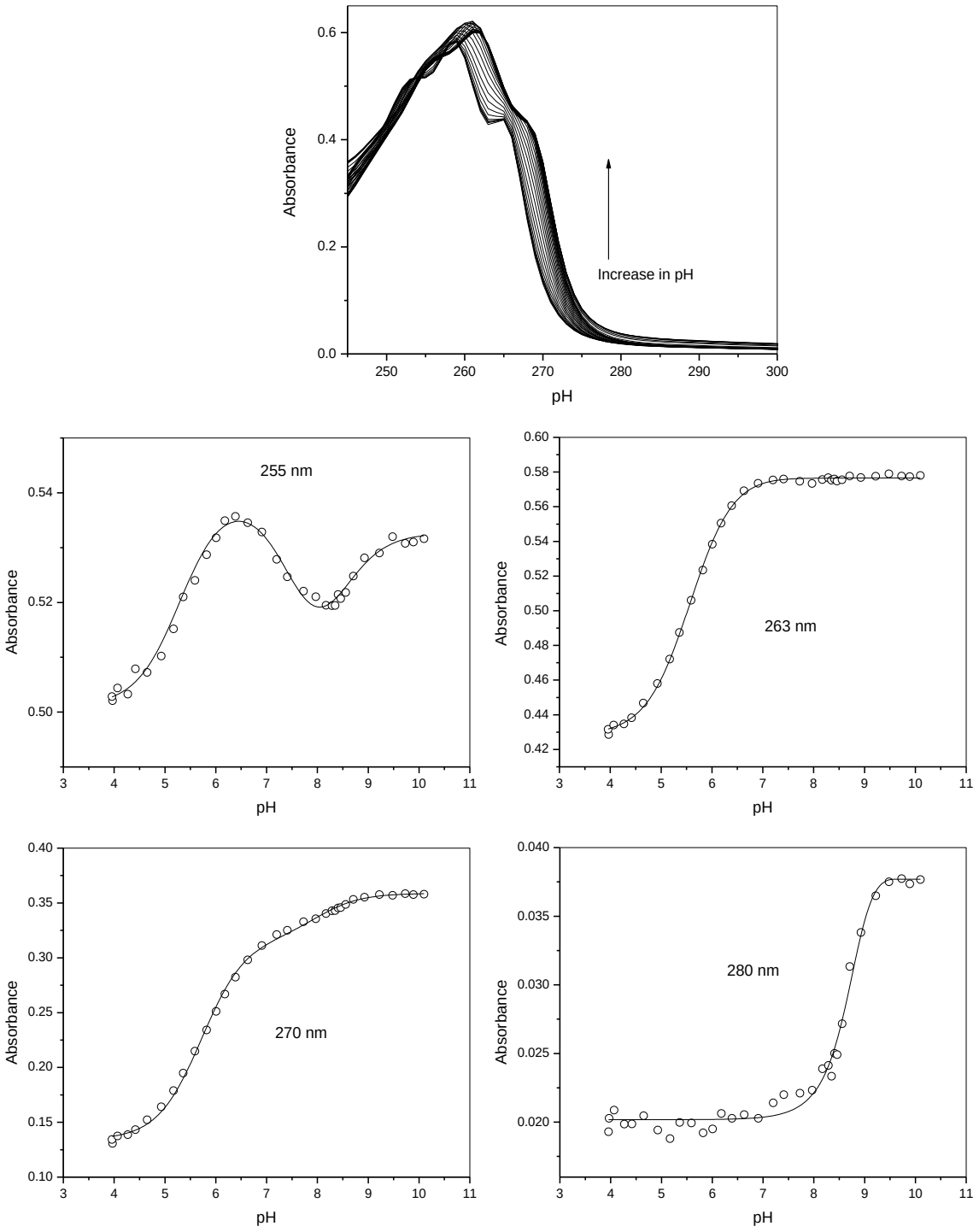

Figure S4. Absorption spectra of the mixture of 0.2 mM **1** and 0.2 mM Zn(II) in the range of pH 4.0-10.1 and plots of absorbance vs. pH at selected fixed wavelengths.

All spectra were exported to Hyperquad program and analyzed quantitatively at 30 wavelengths. Several absorbance vs. pH profiles at wavelengths below, around and above the absorption maximum are shown here for illustrative purposes. In particular, in Figure S2 two clear "waves" reflecting the deprotonation of LH_2^+ form to LH with pK_a 6.96 and LH to L^- with pK_a 11.74 are evident at all wavelengths.

In figure S3 the first wave in fixed-wavelength plots with an inflection point about pH 6.5 reflects the transformation of LH_2^+ to $Cd(LH)^{2+}$. Evidently the coordination to the metal ion affects very little the spectral change induced by deprotonation at this step. The second wave with an inflection point about pH 9.5 reflects the deprotonation of the oxime group of the coordinated ligand with transformation of $Cd(LH)^{2+}$ to $Cd(L)^+$. The spectral change at this step is strongly disturbed by coordination. At shorter wavelengths the absorption goes down rather than up as with the free ligand, but at longer wavelengths it still increases. This titration performed at higher dilution allowed us to make measurements up to pH 10 without precipitation observed in potentiometric titrations about pH 9 and therefore allowed us to determine the pK_a of coordinated oxime group more accurately.

Generally the spectral changes induced by coordination with Zn(II), Figure S4, are similar to those induced by Cd(II), but absorbance vs. pH profiles show more complex behavior in line with larger number of absorbing species in this case. The existence of three deprotonation processes in this case is evident from the profile at 255 nm. The observation of a single wave between pH 8 and 9 at 280 nm, where the major contribution to the change in absorption is due to deprotonation of oxime group, confirms the assignment of pK_a 8.17 to this process rather than to possible formation of a hydroxo complex. Like in a case of Cd(II) spectrophotometric titrations allowed us to follow the complex formation to higher pH values.

Table S1. The overall stability and protonation constants for **1** and its complexes with Zn(II) and Cd(II) (mean values obtained from both potentiometric and spectrophotometric titrations).

Species	logβ
HL	11.74(9)
H_2L	18.7(5)
H_3L	21.3(2)
Zn(HL)	16.78(3)
$Zn(HL)_2$	32.46(3)
Zn(L)	9.40(3)
$Zn(L)H_{-1}$	1.23(2)
Zn(HL)(L)	26.11(4)
Cd(HL)	16.20(3)
Cd(L)	6.83(3)

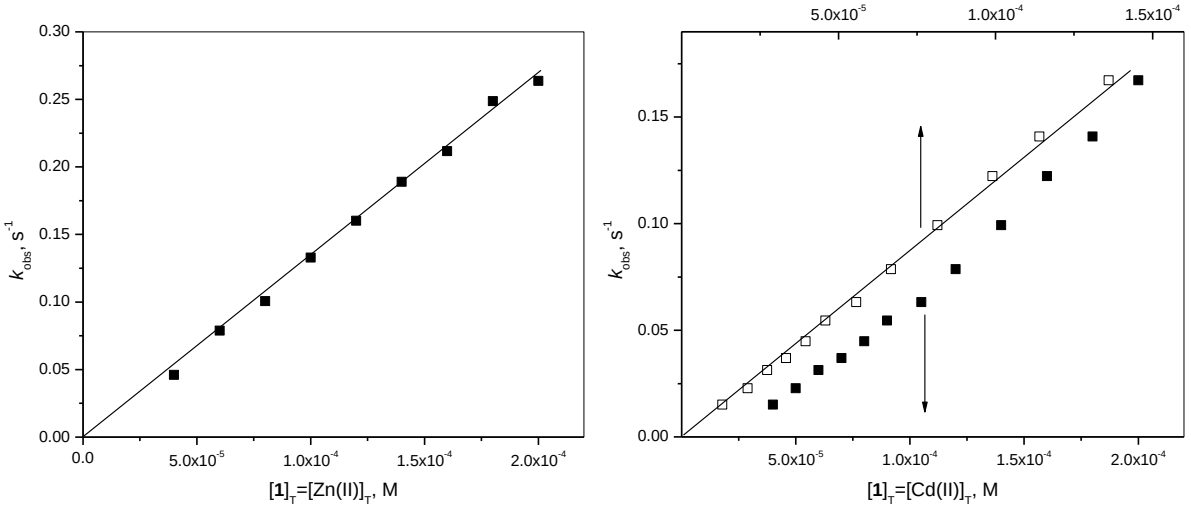

(a) (b)

Figure S5. Observed rate constants for the cleavage of $4x10^{-5}$ M NPA in the presence of equimolar mixtures of oxime **1**and Zn(II) at pH 7.6 (a) or Cd(II) at pH 8.0 (b) in 0.01 M MOPS at 25°C as functions of total concentrations of both components varied at a constant ratio 1:1. In case of Cd(II), which forms less stable complex with **1** the plot has an upward curvature, which disappears when k_{obs} is plotted against calculated concentration of Cd(HL) shown in upper horizontal axis (open squares).

Kinetic studies with an excess of NPA

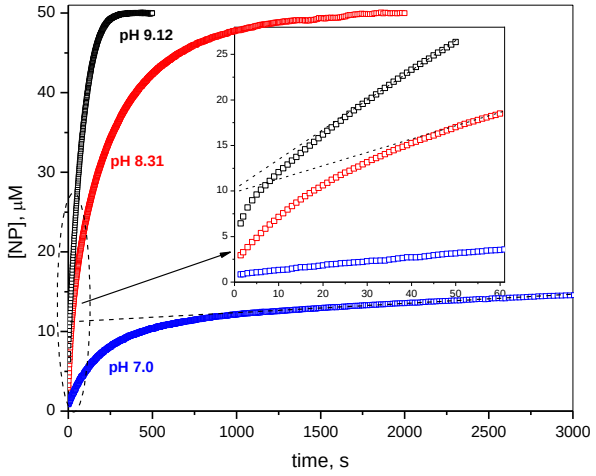

Figure S6. Kinetics of NP formation in the presence of 10 μM **1**, 10 μM Cd(II) and 50 μM NPA at pH 7.0 (blue squares), 8.31 (red squares) and 9.12 (black squares). Inset: expansion of kinetics during the first minute.

Reactions at higher pH values 8.31 and 9.12 proceed to complete hydrolysis of NPA, but do not fit well to simple first-order kinetics. The inset in Figure S1 shows expanded kinetic curves corresponding to the first minute of the reaction. One can clearly see the existence of an initial "burst" in the production of NP followed by a slower reaction. Extrapolation of approximately linear parts of the kinetic curves immediately following the "burst" to zero time gives an intercept equal to the total oximate concentration (dashed lines) indicating the complete acetylation of the oxime at the initial step of the reaction with subsequent slower deacylation, which regenerate the catalysts and allows further NPA cleavage. At low pH 7 the deacylation step becomes very slow and the initial "burst" is more clearly seen (blue points). Expected first-order rate constants of the acylation step at various pH can be estimated as k_{Mox} multiplied by the fraction of metal bound oximate ligand and total NPA concentration assuming the latter to be approximately constant at the initial step of reaction. Calculated rate constants are 0.046, 0.0088 and 2.7×10^{-4} s^{-1} for pH 9.12, 8.31 and 7.0 respectively. They correspond to half-lives of 15, 78 and 2500 s respectively for the "burst" period. Actually observed half-lives are significantly shorter especially at lower pH. The discrepancy probably is due to imprecise calculation of bound ligand fraction at high dilution. Importantly, the kinetics measured with excess of the substrate confirm the acylation-deacylation mechanism outlined in Scheme 1 with very fast acylation step.